Optics Letters

Controllable continuous variable quantum state distributor

Qingwei Wang,[1,†] Yajun Wang,[1,2,†] Xiaocong Sun,[1] Yuhang Tian,[1] Wei Li,[3] Long Tian,[1,2] Xudong Yu,[1,2] Jing Zhang,[1,2,4] and Yaohui Zheng[1,2,*]

[1]State Key Laboratory of Quantum Optics and Quantum Optics Devices, Institute of Opto-Electronics, Shanxi University, Taiyuan 030006, China
[2]Collaborative Innovation Center of Extreme Optics, Shanxi University, Taiyuan, Shanxi 030006, China
[3]College of Physics and Electronic Engineering, Shanxi University, Taiyuan, Shanxi, 030006, China
[4]e-mail: jzhang74@yahoo.com
*Corresponding author: yhzheng@sxu.edu.cn

Received 6 January 2021; revised 1 March 2021; accepted 2 March 2021; posted 3 March 2021 (Doc. ID 419261); published 6 April 2021

To scale quantum information processing, quantum state distributors are an indispensable technology in quantum networks. We present a universal scheme of a continuous variable quantum state distributor that performs point-to-multipoint distributions via quantum teleportation with partially disembodied transport. The fidelity of the state at the output nodes can be conveniently manipulated as needed by engineering the correlation noise of the Einstein–Podolsky–Rosen (EPR) beam. For a 1 → 2 distributor, controllable distributions were demonstrated by manipulating the squeezing factor of EPR entanglement. The fidelities of the two receivers gradually changed from (2/3, 2/3) to (0.95, 0.17) corresponding to the transition from symmetric to asymmetric quantum cloning.

https://doi.org/10.1364/OL.419261

Quantum state distribution is the key ingredient of quantum network and distributed quantum computation [1,2]. It is believed to provide the ultimate solution to the scalability of quantum communication and computation [3]. In general, quantum state distribution refers to the operation in which the information encoded in the states is partially transferred from one system to the others [4–8]. Because of the limitation set by the quantum no-cloning theorem, an unknown quantum state cannot be perfectly replicated [9] and thus prevents deterministic distribution style involving symmetric multidirectional broadcast with high fidelity in the quantum system. Additionally, the limit can be surpassed by abandoning determinism and using probabilistic methods [10,11]. Hence, the deterministic distribution of a quantum state to a desired multipoint is an important challenge for quantum systems, driving intense investigation.

As a burgeoning research area, numerous schemes of quantum state distribution on single photons have been developed [12,13], and optimal quantum distribution based on entangled states has also been proposed [14,15] and demonstrated [16]. However, continuous variable (CV) quantum state distribution is less explored, which is particularly salient for distributed networks of modules [17]. Recently, a CV quantum cloning scheme with linear optics was proposed to realize asymmetric quantum cloning, easily implemented with setups experimentally accessible since only linear optics is required [18]. Yet, in this protocol, most of the information is directly transmitted to the distributor through the quantum channel; therefore, it is vulnerable to potential eavesdropping [19,20]. On the other hand, in stark contrast to a direct channel that suffers from the eavesdropping risk, state teleportation [21–25] was proposed and experimentally demonstrated as a technique for securely transferring an unknown quantum state in virtue of highly entangled states [26,27]. This is a result of the fact that the amount of thermal noise of half of the Einstein–Podolsky–Rosen (EPR) beam is big enough to hide the information of the transmitted state. However, quantum teleportation is limited in point-to-point protocols.

In this Letter, we report an experimental demonstration of a quantum state distributor with controllable fidelity with the assistance of an entanglement state. As a unification of CV quantum teleportation [28,29] and quantum cloning [30–41], the defects aforementioned are overcome. Strikingly, the information in the transmitted channel is enveloped by the usage of the EPR entangled beam [42] while point-to-multipoint distribution is enabled with high fidelities. In addition, the asymmetry of quantum cloning can be manipulated by adjusting the quantum correlation of the EPR beam.

We use the protocol of quantum state transfer with partially disembodied transport to realize the desired quantum state distribution [43], which can be outlined as follows. Generally, quantum states of light can be described by the electromagnetic field annihilation operator $\hat{a}$. The associated amplitude and phase quadratures are written as $\hat{X}=\hat{a}+\hat{a}^\dagger$ and $\hat{Y}=(\hat{a}-\hat{a}^\dagger)/i$, respectively, with the canonical commutator $[\hat{X},\hat{Y}]=2i$. As illustrated in Fig. 1, Sender and Distributor share an EPR entangled beam with $\langle\Delta(\hat{X}_{\mathrm{EPR}_1}+\hat{X}_{\mathrm{EPR}_2})^2\rangle=\langle\Delta(\hat{Y}_{\mathrm{EPR}_1}-\hat{Y}_{\mathrm{EPR}_2})^2\rangle=2e^{-2r}$. An unknown state $\hat{a}_{\mathrm{in}}$ is divided by beam splitter BS1 with variable reflectivity R at the sending station. The reflected output state is combined with Sender's half of the EPR beam $\hat{E}_1$ at a 50/50

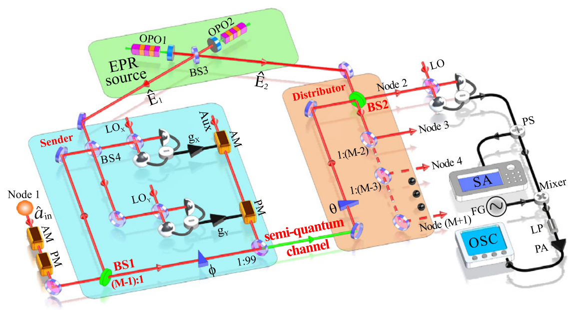

Fig. 1. Schematic of the experimental setup for a CV $1 \to M$ quantum state distributor. An unknown quantum state from node 1 is distributed to M nodes (node 2 to node $(M+1)$). OPO, optical parametric oscillator; BS, beam splitter; AM, amplitude modulator; PM, phase modulator; LO, local oscillator; Aux, auxiliary beam; PS, power splitter; SA, spectrum analyzer; FG, function generator; LP, low-pass filter; PA, pre-amplifier; OSC, oscilloscope.

beam splitter, and then the amplitude $\hat{X}$ and phase $\hat{Y}$ quadratures are measured by two homodyne detectors. In this sense, reflectivity R evaluates the amount of destroyed information of the unknown quantum state. The extracted information from homodyne detection is encoded in an auxiliary beam via two independent modulators with scaling factors g_X and g_Y. The transmitted output of BS1 is displaced by such an auxiliary beam by means of 1/99 optical interference. The displaced state $\hat{a}_{\text{disp}}$ is then transmitted to Distributor through the semi-quantum channel. After receiving the information from Sender, Distributor reconstructs the unknown state by interfering with the displaced field using his entangled beam $\hat{E}_2$ at another beam splitter BS2 with the same reflectivity R.

State transfer is generally evaluated by the fidelity, determined by the overlap between input state $|\psi_{\text{in}}\rangle$ and output state $|\psi_{\text{out}}\rangle$, i.e., $F = \langle\psi_{\text{in}}|\hat{\rho}_{\text{out}}|\psi_{\text{in}}\rangle$, with density matrix $\hat{\rho}_{\text{out}} = |\psi_{\text{out}}\rangle\langle\psi_{\text{out}}|$. In the scheme presented here, the value of fidelity F is associated with squeezing degree r and relative phase θ, and thus for convenience, we define a parameter $V(r, \theta) = e^{-2r} \cos^2 \frac{\theta}{2} + e^{2r} \sin^2 \frac{\theta}{2}$ to formulate the fidelity (see Section 2 of Supplement 1). As stated above, this protocol is a unification of quantum teleportation and quantum cloning: (1) $R = 1$—it is equivalent to standard quantum teleportation with fidelity $F = \frac{1}{1+V(r,\theta)}$ ranging from 0.5 to one, as shown in Fig. 2(b); (2) $R = 1/2$—$1 \to 2$ symmetric and asymmetric Gaussian cloning can be realized [Fig. 2(c)]. In the absence of an entanglement source ($r = 0$, $V(r, \theta) = 1$), the two output nodes have the same fidelities of 2/3, corresponding to symmetric Gaussian cloning. However, when $V(r, \theta) < 1$, the fidelity at one of the outputs (here assumed to be node 2) on BS2 is $F = \frac{2}{2+V(r,\theta)}$, obviously larger than 2/3. At this moment, the other output (node 3) on BS2 has a phase $\pi + \theta$ of EPR2 relative to the displaced beam. Moreover, the fidelity $F = \frac{2}{2+V(r,\theta+\pi)}$ at the output is less than 2/3, with no violation of the no-cloning theorem. Interestingly, with $\theta = 0$, the fidelity at node 2 (node 3) changes from 2/3 to one (zero) as squeezing factor r increases to infinity. On the contrary, the fidelities of node 2 and node 3 are inversed when $\theta = \pi$. Thus, one can manipulate the fidelities at two output nodes with an arbitrary value from zero to one by the combined control of r and θ in ideal conditions. Furthermore, together with $(M - 2)$ beam splitters, the setup can be extended to the $1 \to M$ optimal

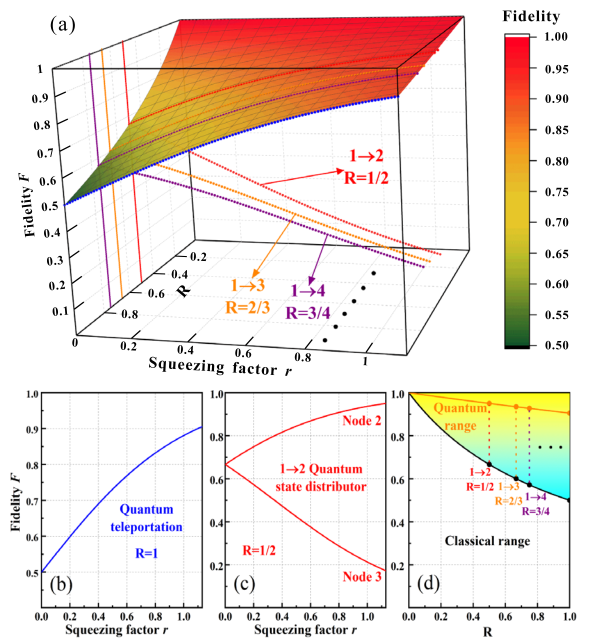

Fig. 2. (a) Dependence of distributed state fidelity on the squeezing factor, and the reflectivity R of BS1 and BS2. (b) Cross-section of (a) for $R = 1$, corresponding to quantum teleportation. (c) Cross-section of (a) for $R = 1/2$, corresponding to the $1 \to 2$ quantum state distributor. (d) Fidelity of the quantum state distributor as a function of reflectivity R; orange line: fidelity in the quantum range could be achieved by our setup.

quantum state cloning by simply replacing R with $(M - 1)/M$. Similarly, the fidelity at each node can be manipulated by r and θ, and the fidelities at node 4 to node $(M + 1)$ are the same as that of node 3. Therefore, controllable CV point-to-multipoint quantum state distributors can be realized with our scheme. We emphasize that by increasing reflectivity R, the proportion of the thermal noise of entanglement becomes higher; consequently, the potential eavesdropper could get less information of the transmitted quantum state from the semi-quantum channel (see Section 5 of Supplement 1). It is the main advantage of the introduction of EPR entanglement.

Experimentally, an EPR entangled beam is generated by combining two independent squeezed beams at a 50/50 beam splitter, with the relative phase $\pi/2$ between the squeezed fields actively servo-controlled. The squeezed fields are produced by a sub-threshold optical parametric oscillator (OPO) with periodically poled $KTiOPO_4$ (PPKTP). With technical improvements in phase noise [44–46], system loss [47,48], and detector dark noise [49,50], the maximum squeezing level is measured at 13.8 dB below the shot noise limit (SNL) at 1064 nm. Notice that weak coherent beams are injected into two OPOs as probe beams that provide cavity- and phase-locking. Finally, the EPR beam with $\langle\Delta(\hat{X}_{\text{EPR}_1} + \hat{X}_{\text{EPR}_2})^2\rangle = -11.3 \pm 0.2$ dB and $\langle\Delta(\hat{Y}_{\text{EPR}_1} - \hat{Y}_{\text{EPR}_2})^2\rangle = -11.1 \pm 0.2$ dB is obtained serving as the key building block of the presented scheme. As shown in Fig. 1, EPR beam 1 propagates to the sending station, where it is combined at a 50/50 beam splitter with the reflected part of the unknown input state $\hat{a}_{\text{in}}$ (coherent state, encoded by amplitude and phase modulators). Then the measured information with two-homodyne detection is fed back to the transmitted part of $\hat{a}_{\text{in}}$ by means of interference of the modulated auxiliary beam with the transmitted output of BS1 with the relative phase $\phi = 0$. This displaced beam is sent to the distributing station through the semi-quantum channel, where Distributor reconstructs the unknown state by interfering with the transmitted optical field using his entangled beam $\hat{E}_2$ at another beam splitter BS2 with relative phase θ. Note that all the relative phases, including the beam combination and quadrature component detection, are actively stabilized during the measurement cycle via the Pound–Drever–Hall locking technique, and phase θ is locked to zero or π, which is dependent on the desired fidelity of the distributed quantum state between the two outputs of BS2. In addition, output node 3 of BS2 can be sent to a single user to perform two-path quantum state distribution and also through multiple beam splitters to perform a multi-path distribution. Actually, imperfections inevitably exist in the distributor to deteriorate fidelity, which are attributed mainly to phase fluctuations, losses, and excess noises in the state's preparation, modulation, transmission, and detection processes.

For $R = 1$, quantum teleportation has been experimentally verified [25], and here we perform a controllable point-to-two-point quantum state distribution experimentally by setting $R = 1/2$. To assess the quality of the CV quantum state distributor, the gains for the amplitude and phase information are carefully calibrated [Fig. 3(a)], and the noise power of the distributed state at node 2 and node 3 is measured at optimal $V(r, \theta)$ ($r = 1.128, \theta = 0$) to obtain the optimal fidelities at the two nodes; the results are shown in Fig. 3(b). SNL is measured with only the local oscillator entering the detector. With the pump beams of the two OPOs blocked, the outputs from BS1 are not quantum correlated. The noise power of the distributed state corresponds to the classical limit, which is the best achievable value in the absence of an EPR entangled beam. In this case, the two output states at node 2 and node 3 have the same fidelity of 2/3, which sets a boundary for entrance into the quantum domain. In the presence of an EPR entangled beam, the noise power of the distributed states at node 2 and node 3 are measured at optimal $V(r, \theta)$. The measured values are 2.6 ± 0.2 dB below the noise level of the corresponding classical boundary, and 7.2 ± 0.2 dB above that of the classical boundary [Fig. 3(b)]. The fidelities at the two output nodes that were inferred from the fidelity expression are 0.95 (node 2) and 0.17 (node 3). Furthermore, we measured the noise power of the distributed states at $r = 1.128, \theta = \pi$ [Fig. 3(c)]. All the results are the same as those in Fig. 3(b) except for the noise power switchover between the two nodes.

While varying squeezing factor r, the noise powers of the two nodes with $\theta = 0$ are measured. Figure 4(a) shows the fidelities inferred from the noise power measurements. It is found that the fidelity at node 2 (node 3) changes from 2/3 to 0.95 (0.17), as r increases. The squeezing factor can be conveniently controlled between zero and 1.128 by changing the pump power of the OPOs (see Section 1 of Supplement 1).

Furthermore, we also measured the noise power of the two nodes as a function of phase θ with fixed squeezing factor r [Fig. 4(b)]. Clearly, by varing θ, the fidelities at the two nodes switch back and forth with phase during the distribution. Due to the existance of an additional phase delay of π at node 3 with respect to node 2, the fidelities at the two outputs of BS2 are relevant but different. In combination with controlling squeezing factor r, we manipulate the controllable fidelity from 0.17 to 0.95 at each distributed node. When the fidelity at one of the

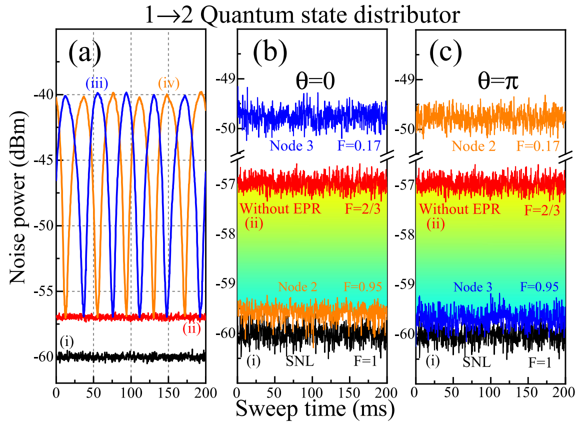

Fig. 3. (a) Noise powers recorded at node 2 while scanning the phase of the input beam without EPR entanglement: trace (i) is the shot noise limit; trace (ii) shows the teleported state for a vacuum input without EPR entanglement; trace (iii) and trace (iv) show the recreation of input coherent modulation amplitude of 20 dB, demonstrating that the peak input and output amplitudes are equal, and the amplitude and phase quadratures are indeed $\pi/2$ apart in phase. (b) Distributed state for a vacuum input with EPR entanglement ($R = 1/2, \theta = 0, \theta$ is the phase of EPR2 relative to the auxiliary beam). (c) Distributed state for a vacuum input with EPR entanglement ($R = 1/2, \theta = \pi$).

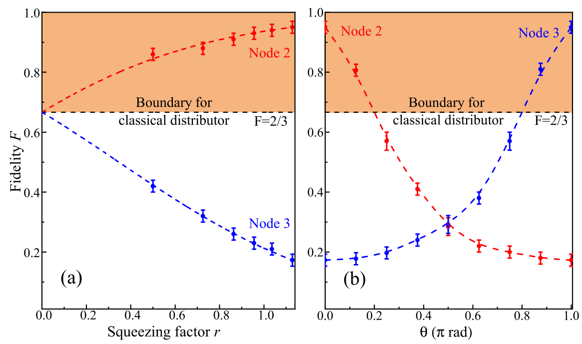

Fig. 4. Fidelities at node 2 and node 3 as a function of squeezing factor of the correlation variance $V(r, \theta)$ ($1 \to 2$ quantum state distributor). (a) With the squeezing factor manipulated, $\theta = 0$; (b) with θ scanned, $r = 1.128$. The error bars are acquired during 20 measurements.

two nodes is more than the classical boundary 2/3, the fidelity at the other node must be less than this classical boundary without violating the no-cloning limit. However, in the presented controllable distribution process, by tuning squeezing factor r and θ at the desired time, high-fidelity quantum state distribution is feasible at each of the two nodes, thereby functioning as a $1 \to 2$ distributor of quantum information. By optimizing $V(r, \theta)$ to reach the minimum value, the distributed quantum state has the best achievable fidelity.

In conclusion, we have reported an experimental realization of unifying the CV point-to-multipoint quantum state distributions via quantum teleportation with partially disembodied transport. By setting values of reflectivity R for BS1 and BS2, the functionality of the setup can be conveniently switched. In either case, the fidelity at the output nodes can be adjusted within limits as needed by manipulating the parameter $V(r, \theta)$

with regard to EPR entangled states. The fidelity at only one of the nodes may exceed the classical boundary, with no violation of the no-cloning theorem. Strikingly, the information of the transmitted quantum state is submerged in the thermal noise of the highly entangled state with the introduction of the entangled states. By virtue of the controllable distribution process, the quantum state for which the fidelity rises above the classical boundary is capable of a time-sharing operation at the two nodes, thereby functioning as a $1 \to 2$ distributor of quantum information for a distributed quantum network and quantum computer. Together with $(M-2)$ beam splitters, the setup can also be extended to a $1 \to M$ optimal quantum state distribution by simply changing R to $(M-1)/M$. With $R = 1/2$, we succeeded in obtaining an optimal fidelity of $F = 0.95$ with a coherent state as an input state. Owing to high fidelity, the scheme can also be scalable to 2^9 distribution nodes by a cascaded distribution operation with the ultimate fidelity beyond the classical limit 2/3 (see Section 4 of Supplement 1). This work introduces a new route to exploring the CV multiple-point quantum state distributor and advanced quantum operations by means of CV quantum state transport protocols. Furthermore, the reversibility of CV quantum cloning could be implemented by upgrading our setup [19,39], which will prompt the protocol applied to the multiple-point to multiple-point connecting, quantum interface [51], and quantum transducers.

Funding. National Natural Science Foundation of China (11654002, 11804206, 11804207, 11874250, 62027821, 62035015); National Key Research and Development Program of China (2020YFC2200402); Key R&D Projects of Shanxi Province (201903D111001); Program for Sanjin Scholar of Shanxi Province; Program for Outstanding Innovative Teams of Higher Learning Institutions of Shanxi; Fund for Shanxi "1331 Project" Key Subjects Construction.

Disclosures. The authors declare no conflicts of interest.

Data Availability. Data underlying the results presented in this paper are not publicly available at this time but may be obtained from the authors upon reasonable request.

Supplemental document. See Supplement 1 for supporting content.

†These authors contributed equally to this Letter.

REFERENCES

1. J. I. Cirac, P. Zoller, H. J. Kimble, and H. Mabuchi, Phys. Rev. Lett. **78**, 3221 (1997).
2. I.-C. Hoi, C. M. Wilson, G. Johansson, T. Palomaki, B. Peropadre, and P. Delsing, Phys. Rev. Lett. **107**, 073601 (2011).
3. H. J. Kimble, Nature **453**, 1023 (2008).
4. S. L. Braunstein, V. Bužek, and M. Hillery, Phys. Rev. A **63**, 052313 (2001).
5. S. L. Braunstein and P. van Loock, Rev. Mod. Phys. **77**, 513 (2005).
6. E. Nagali, L. Sansoni, F. Sciarrino, F. D. Martini, L. Marrucci, B. Piccirillo, E. Karimi, and E. Santamato, Nat. Photonics **3**, 720 (2009).
7. H. Fan, Y. Wang, L. Jing, J. Yuea, H. Shi, Y. Zhang, and L. Mu, Phys. Rep. **544**, 241 (2014).
8. M. Ricci, F. Sciarrino, N. J. Cerf, R. Filip, J. Fiurášek, and F. D. Martini, Phys. Rev. Lett. **95**, 090504 (2005).
9. W. K. Wootters and W. H. Zurek, Nature **299**, 802 (1982).
10. C. R. Müller, C. Wittmann, P. Marek, R. Filip, C. Marquardt, G. Leuchs, and U. L. Andersen, Phys. Rev. A **86**, 010305 (2012).
11. J. Y. Haw, J. Zhao, J. Dias, S. M. Assad, M. Bradshaw, R. Blandino, T. Symul, T. C. Ralph, and P. K. Lam, Nat. Commun. **7**, 13222 (2016).
12. I. Shomroni, S. Rosenblum, Y. Lovsky, O. Bechler, G. Guendelman, and B. Dayan, Science **345**, 903 (2014).
13. M. A. Hall, J. B. Altepeter, and P. Kumar, Phys. Rev. Lett. **106**, 053901 (2011).
14. R. Filip, Phys. Rev. A **69**, 032309 (2004).
15. R. Filip, Phys. Rev. A **69**, 052301 (2004).
16. Z. Zhao, A. N. Zhang, X. Q. Zhou, Y. A. Chen, C. Y. Lu, A. Karlsson, and J. W. Pan, Phys. Rev. Lett. **95**, 030502 (2005).
17. K. S. Chou, J. Z. Blumoff, C. S. Wang, P. C. Reinhold, C. J. Axline, Y. Y. Gao, L. Frunzio, M. H. Devoret, L. Jiang, and R. J. Schoelkopf, Nature **561**, 368 (2018).
18. Z. Zhai, J. Guo, and J. Gao, Phys. Rev. A **73**, 052302 (2006).
19. R. Filip, J. Fiurášek, and P. Marek, Phys. Rev. A **69**, 012314 (2004).
20. (De), R. Demkowicz-Dobrzański, A. Sen, U. Sen, and M. Lewenstein, Phys. Rev. A **80**, 012311 (2009).
21. D. Bouwmeester, J.-W. Pan, K. Mattle, M. Eibl, H. Weinfurter, and A. Zeilinger, Nature **390**, 575 (1997).
22. S. Takeda, T. Mizuta, M. Fuwa, P. van Loock, and A. Furusawa, Nature **500**, 315 (2013).
23. X. L. Wang, X. D. Cai, Z. E. Su, M. C. Chen, D. Wu, L. Li, N. L. Liu, C. Y. Lu, and J. W. Pan, Nature **518**, 516 (2018).
24. W. Pfaff, B. J. Hensen, H. Bernien, S. B. van Dam, M. S. Blok, T. H. Taminiau, M. J. Tiggelman, R. N. Schouten, M. Markham, D. J. Twitchen, and R. Hanson, Science **345**, 532 (2014).
25. A. Furusawa, J. L. Søurensen, S. L. Braunstein, C. A. Fuchs, H. J. Kimble, and E. S. Polzik, Science **282**, 706 (1998).
26. M. V. Larsen, X. Guo, C. R. Breum, J. S. Neergaard-Nielsen, and U. L. Andersen, npj Quantum Inf. **5**, 46 (2019).
27. T. Eberle, V. Händchen, and R. Schnabel, Opt. Express **21**, 11546 (2013).
28. W. P. Bowen, N. Treps, B. C. Buchler, R. Schnabel, T. C. Ralph, H. Bachor, T. Symul, and P. K. Lam, Phys. Rev. A **67**, 032302 (2003).
29. U. L. Andersen and T. C. Ralph, Phys. Rev. Lett. **111**, 050504 (2013).
30. V. Scarani, S. Iblisdir, and N. Gisin, Rev. Mod. Phys. **77**, 1225 (2005).
31. J. Fiurášek, Phys. Rev. Lett. **86**, 4942 (2001).
32. U. L. Andersen, V. Josse, and G. Leuchs, Phys. Rev. Lett. **94**, 240503 (2005).
33. M. Ricci, F. Sciarrino, C. Sias, and F. D. Martini, Phys. Rev. Lett. **92**, 047901 (2004).
34. K. Bartkiewicz, K. Lemr, A. Cernoch, J. Soubusta, and A. Miranowicz, Phys. Rev. Lett. **110**, 173601 (2013).
35. L. Bartůšková, M. Dušek, A. Černoch, J. Soubusta, and J. Fiurášek, Phys. Rev. Lett. **99**, 120505 (2007).
36. M. Guţă and K. Matsumoto, Phys. Rev. A **74**, 032305 (2006).
37. S. Iblisdir, A. Acín, N. J. Cerf, R. Filip, J. Fiurášek, and N. Gisin, Phys. Rev. A **72**, 042328 (2005).
38. J. Fiurášek and N. J. Cerf, Phys. Rev. A **75**, 052335 (2007).
39. J. Zhang, C. Xie, and K. Peng, Phys. Rev. A **73**, 042315 (2006).
40. S. Koike, H. Takahashi, H. Yonezawa, N. Takei, S. L. Braunstein, T. Aoki, and A. Furusawa, Phys. Rev. Lett. **96**, 060504 (2006).
41. J. Yoshikawa, Y. Miwa, R. Filip, and A. Furusawa, Phys. Rev. A **83**, 052307 (2011).
42. Z. Chen, Q. Zhang, X. Bao, J. Schmiedmayer, and J. Pan, Phys. Rev. A **73**, 050302 (2006).
43. J. Zhang, C. Xie, and K. Peng, Phys. Rev. Lett. **95**, 170501 (2005).
44. W. Yang, S. Shi, Y. Wang, W. Ma, Y. Zheng, and K. Peng, Opt. Lett. **42**, 4553 (2017).
45. K. McKenzie, N. Grosse, W. P. Bowen, S. E. Whitcomb, M. B. Gray, D. E. McClelland, and P. K. Lam, Phys. Rev. Lett. **93**, 161105 (2004).
46. Y. Takeno, M. Yukawa, H. Yonezawa, and A. Furusawa, Opt. Express **15**, 4321 (2007).
47. S. Shi, Y. Wang, W. Yang, Y. Zheng, and K. Peng, Opt. Lett. **43**, 5411 (2018).
48. M. Mehmet, S. Ast, T. Eberle, S. Steinlechner, H. Vahlbruch, and R. Schnabel, Opt. Express **19**, 25763 (2011).
49. X. Sun, Y. Wang, L. Tian, Y. Zheng, and K. Peng, Chin. Opt. Lett. **17**, 072701 (2019).
50. M. S. Stefszky, C. M. Mow-Lowry, S. S. Y. Chua, D. A. Shaddock, B. C. Buchler, H. Vahlbruch, A. Khalaidobski, R. Schnabel, P. K. Lam, and D. E. McClell, Class. Quantum Graviy **29**, 145015 (2012).
51. R. Filip, Phys. Rev. A **80**, 022304 (2009).